Indian Journal of Biochemistry & Biophysics
Vol. 58, April 2021, pp. 135-140

Hierarchical gold nanostructures based sensor for sensitive and fast detection of cancer biomarker

Samriddhi Mehta[1,4], Shrishty Bakshi[1], Sangeeta Choudhury[2], Sudeep Bose[3,5]* & Ranu Nayak[1]*

[1]Amity Institute of Nanotechnology; [3]Amity Institute of Biotechnology; & [5]Amity Institute of Molecular Medicine & Stem Cell Research, Amity University, Noida-201 313, Uttar Pradesh, India

[2]Research Department, Sir Ganga Ram Hospital, New Delhi-110 060, Delhi, India

[4]Translational Health Science and Technology Institute, Faridabad-121 001, Haryana, India

Received 02 January 2020; *revised 17 August 2020*

Importance of precision diagnostics in healthcare has been ignited by the idea that early detection of cancer would immensely benefit patients in terms of more effective and timely treatment modality. Clinical samples in the form of biopsy specimen/serum/urine/saliva contains an ocean of diagnostic information to generate conclusive information for more precise and evidence-based options to manage cancer. However, to achieve this, there is a need detect biomarkers, that can provide significantly increased diagnostic accuracy. Nanobiosensors have undoubtedly boomed to claim ultrasensitive detection of DNA cancer biomarkers in attomolar and femtomolar range. However, ultrasensitive and accurate detection of protein biomarker is rare. This work describes fabrication of a hierarchical gold nano-biosensor (HAu) for ultra-sensitive detection of cancer protein biomarkers in pg/mL range. Unique chemical modification during electrochemical synthesis has rendered highly uniformed and dense nanostructures of gold on a solid platform. Factors affecting homogeneity and sensitivity of the sensing platform have been optimized in detail. Voltammetric sensing based on antibody-antigen interaction on the given sensing platform has demonstrated a wide linear range of detection for EGFR varying from 10 pg/mL to 1 ng/mL concentration.

Keywords: Electrochemical detection, Gold nanostructure, Immunosensor, Protein marker

Sensitive and accurate detection of biomarkers is of utmost importance and demand, especially for early detection, diagnosis and treatment of any diseases[1,2]. Biomarkers can be a protein, DNA/RNA, or any other biomolecule[3,4]. Measurement of protein biomarker is a promising way to derive information regarding risk factor of a given disease or permit early detection of disease for better treatment modality[5,6]. These biomarkers are often present in trace levels mixed with various other proteins, making the procedure quite laborious[7,8]. Despite the ordeals, there has been huge progress in the field of biomarker detection technologies and numerous target specific biomarker detection methods have been developed.

The present scenario for screening and detection of discrete biomarkers is based on the use of enzyme-linked immunosorbent assay (ELISA), target specific bioassays, and Next Generation Sequencing (NGS) along with, yet evolving tools like DNA chips/ microarrays[9]. Although these techniques are established and sensitive, they are expensive, technically burdensome, and time-consuming methods[10]. Since there is no universal ultrasensitive enzymatic amplification method for proteins like polymerase chain reaction (PCR) or microarray for the detection of nucleic acid, thus a diagnostic tool with ultra-sensitivity (pM, fM concentration or lower) and specificity is highly required.

In recent years, enhancements in the field of biomolecule detection treatment have taken advantage of the burgeoning use of nanomaterials to create novel nanobiosensors[11,12]. Generally, nano-biosensors are based on nanoparticles that are conjugated to a specific targeting ligand. The specificity is brought about by ligand, which tends to binds to the particular marker or protein of interest. Nano-biosensors usually because of higher biocompatibility, sensitivity and specificity show dramatic supremacy over most conventional detection kits and sensing systems[13]. Especially, the biosensors that rely on electrochemical signals to detect quantitative variation in bio-analyte[14]. An electrochemical sensor couples a bio-receptor (*e.g.* protein, DNA) to a transducer surface to convert a biological correspondence (*e.g.* antibody-antigen interaction, complimentary hybridization) into a measurable current signal. Tremendous efforts have been put forward on the

*Correspondence:
Phone: +91-9818936883; +91-8800690946 (Mob)
E-mail: sbose1@amity.edu (SB); rnayak@amity.edu (RN)

realization of electrochemical biosensors for detection of biomarkers at both protein and DNA level[15].

Amongst various nanomaterials, gold nanoparticles/ nanostructures have attracted an enormous amount of interest for biological sensing applications. Gold nanoparticles have unique optical, physical and catalytic properties that include high electrical conductivity, reflectivity, and easy surface functionalization for conveniently adhering desired the bio-analyte[16-19]. Gold is also non-reactive and relatively inert which makes it good for *in vivo* and *in vitro* analysis of biomolecules[20]. Furthermore, low cytotoxicity and high biocompatibility of gold has been demonstrated by a number of clinical studies, making it an ideal substrate for immunosensor fabrication[20–22]. Several efforts in the development and performance augmentation of gold nanostructures as sensitive and selective biosensor have recently surface[23-26].

Gold nanostructure assisted nanobiosensors can be the next generation tool for rapid and enhance disease detection. However, there is still ample scope for improvement in the biosensing technology; hence there is a need to reassess the strategies to detect low concentrations of biomarkers meanwhile also taking care of false positive results. Stable and uniform immobilization of antibodies onto a sensing surface without altering their specificity and immunological activity is the other crucial aspect of nano-biosensor fabrication. Non-homogeneity in immobilization may strongly affect the detection limit, sensitivity, repeatability and thereby hampering overall sensor performance in real-time[27]. Not many efforts have been made to see the effect of surface roughness, homogeneous coverage of nanostructures in a biosensor[28]. In this work, we have emphasized on intensifying surface roughness and surface coverage of immunoassay-biosensor along with ameliorating homogeneity in protein immobilization for ultrahigh sensitivity of detection. A 3D hierarchically nanostructured gold electrode (HAu) has been prepared by a simple electrodeposition methodology, extensively optimized to obtain uniform growth of the nanostructure. This platform can be potentially utilized for protein/ DNA biomarkers for cancer. EGFR is a protein that is often upregulated in various types of cancer. As a prototype, here EGFR is detected using antigen-antibody interaction and its dynamic range of detection has been evaluated.

Materials & Methods

Materials & Reagents

Gold coated 1" × 3" glass slide, Bradford's reagent (from Thermo Scientific); Platinum (Pt) mesh electrode; Ag/AgCl electrode (CH Instruments Inc.); $HAuCl_4.3H_2O$ salt, Sodium phosphate monobasic and dibasic, Potassium ferrocyanide and ferricyanide , 3-Aminopropyl triethoxysilane, 11-Mercaptoundecanoic acid (MUA), *N*-(3-Dimethylaminopropyl)-*N*′ -ethyl-carbodiimide hydrochloride (EDC), *N*-Hydroxy-succinimide (NHS), and Bovine serum albumin (BSA) (from Sigma Aldrich), Epithelial Growth factor receptor (EGFR) Rabbit monoclonal Antibody (Cell Signaling Technology), EGFR Protein, Human, Recombinant (Sino Biological). All chemicals and solvents used were of Analytical grade.

Electrodeposition of hierarchical gold (HAu) sensing electrode

Electrochemical remodeling of a plain gold surface to obtain the 3D hierarchical surface was achieved using EmStat3+ potentiostat (PalmSens BV, Netherlands). A three electrode cell with Platinum (Pt) mesh counter electrode, Ag/AgCl electrode reference electrode and gold/ glass (0.7 cm × 0.7 cm – active area) in presence of 2 mg/mL $HAuCl_4$ in 0.2 M H_2SO_4 electrolyte solution with 0.2% *v/v* APTES was used for effectuating growth[27]. Linear sweep voltammetry (LSV) was performed between − 0.8 to − 0.2 V potential with a scan rate of 0.01 V/s and electrodeposition was performed up to accumulation of 30 Coulomb charge.

Surface functionalization of HAu

Hierarchical gold (HAu) electrode was dipped in a 10 mM ethanolic solution of MUA for 45 min followed by thorough rinsing in ethanol. Thereafter, the –COOH functionalized HAu electrode was activated by a mixture of 80 mM NHS and 80 mM EDC and incubated for 55 min at room temperature.

Protein estimation using Bradford assay

Standard calibration curve of BSA was prepared using a protein stock solution of 2 mg/mL in 0.1 M PBS and its desired dilutions. Optical density measurement was done at 595 nm wavelength. in order to estimate amount of bound protein on the HAu electrode surface, 25 µg of BSA was incubated for 2 h on the –COOH functionalized HAu electrode. Incubation was followed by washing (5 times using 0.1 M PBS), the wash buffer was collected and stored for bound protein estimation. The experiment was repeated 3 times on 3 sets of electrodes – plain gold electrode with surface functionalization, HAu electrode with surface functionalization, and HAu electrode without surface functionalization. Optical density was measured at 595 nm on each set of

collected wash buffer for estimation of unbound protein, thus, knowing the bound protein on the sensing surface.

Antibody - Antigen immunosensing on surface functionalized HAu electrode

EGFR immunoglobulin (Antibody) of 500 ng/mL concentration was incubated onto the -COOH activated HAu electrode for 2 h at room temperature. Different concentrations of EGFR recombinant protein solutions ranging from 1 ng/mL to 10 pg/mL was interacted with the immobilized immunoglobulin molecules on the HAu electrode at room temperature for 2 h followed by Cyclic voltammetry analysis.

Results and Discussion

Formation of HAu electrode

HAu electrode was electrodeposited by Linear sweep voltammetry (LSV). During electrodeposition, plain gold surface morphology transforms from lustrous golden to rough dark brown colour. A distinct difference in the conductivity of the resultant HAu electrode was observed as shown in the cyclic voltammogram (CV) in (Fig. 1). Redox activity was significantly improved in comparison to that of a plain electrode. It is observed from (Fig. 1) that plain gold electrode's oxidative peak current is at 236 µA; whereas that for HAu electrode is as high as 1779 µA. The apparent reason for increase in the peak current and overall the integral area of the CV is the increase in surface area of the gold electrode on transformation to micro/nanostructured surface. Use of optimum amount of APTES further enhanced the conductivity of HAu electrode by almost 8 fold.

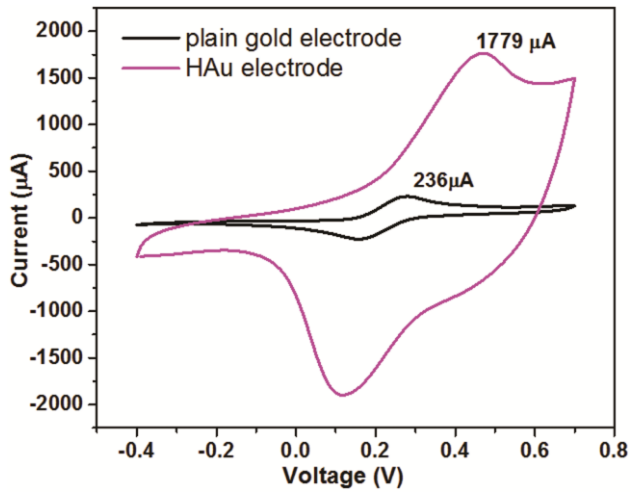

Fig. 1 — Comparison of CV of equimolar $[Fe(CN)_6]^{-3/-4}$ in KCl using plain gold and HAu electrode

Surface morphology of the HAu electrode was observed by SEM. Figure 2 shows a predominant growth of 3D hierarchical gold micro/nanostructures on the electrode. It can be seen from (Fig. 2) inset that the nanostructure dimension is around 300 nm × 200 nm. The nanostructures look quite homogeneously distributed That is most likely to promote uniform immobilization of biomolecules and hence endorse higher reproducibility of a biosensor.

Surface functionalization of HAu electrode for covalent binding of protein

Optimum surface modification sturdy and reliable enough to facilitate strong protein clamping onto the electrode sensing area is indispensable to a protein detecting biosensor design. Covalent binding of protein using self-assembled monolayers of organic molecules is a promising method. A well known surface chemistry was used by binding MUA on the gold electrode surface through thiol linkage (-SH), simultaneously keeping the carboxyl end facing towards the exterior side. Thereafter, the electrode was reacted with EDC and NHS to activate the –COOH linkage for strong binding of protein via –CO-NH (amide) bond formation, CV was measured after every consecutive step of surface modification and is shown in (Fig. 3). A distinct reduction in the redox peaks was observed upon MUA treatment.

Further, slight suppression of the redox peaks was again observed on addition of EDC-NHS on the MUA treated sensing surface. It hindered the interaction of the gold nanostructures with the $Fe(CN)_6^{3-/4-}$ thus, showing lower redox activity. Finally, on BSA protein immobilization, the redox peaks were seen to significantly get suppressed, demonstrating the isolating nature of BSA protein.

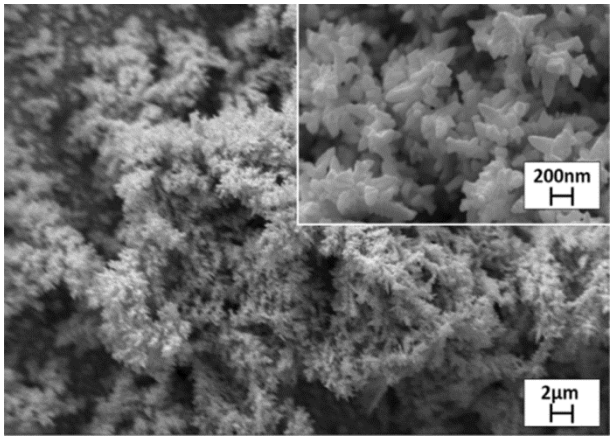

Fig. 2 — SEM image of as prepared HAu electrode. Note: Inset showing high magnification image

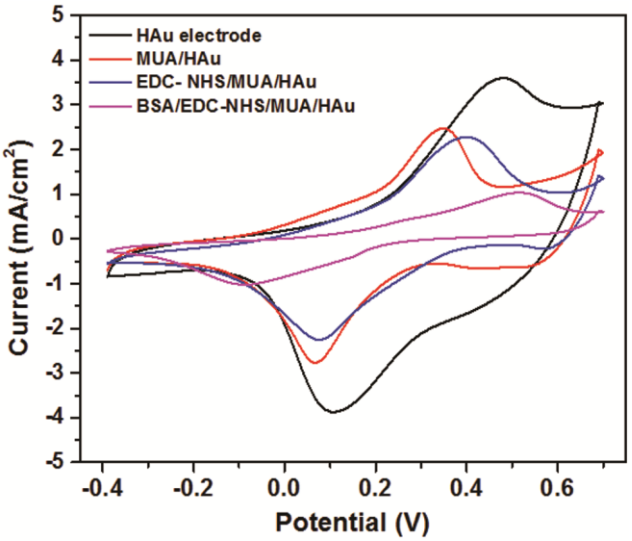

Fig. 3 — CV of equimolar $[Fe(CN)6]^{-3/-4}$ in KCl using HAu electrode immobilized with BSA protein

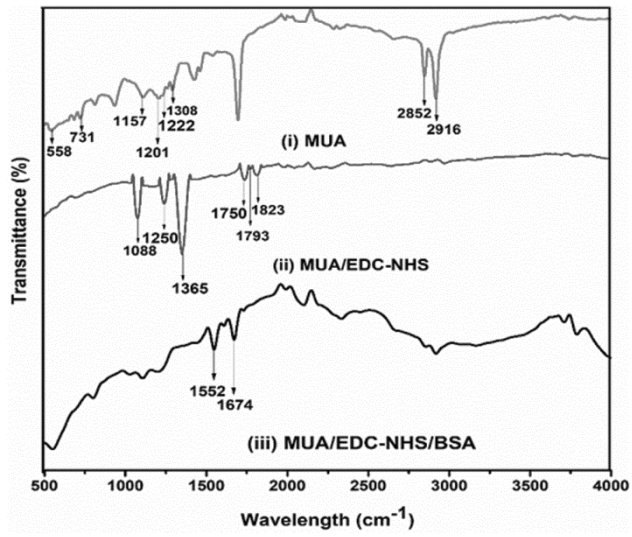

Fig. 4 — FTIR spectra of HAu electrode chemically modifications using (i) MUA; (ii) EDC-NHS; (iii) BSA protein

Formation of monolayers of MUA, EDC-NHS on HAu electrode followed by covalent binding of protein was also validated by FTIR spectroscopy. Figure 4 shows the IR spectra of MUA and EDC-NHS functionalized HAu electrode followed by protein immobilization. The peaks were identified using previous literatures[30-32]. In brief, attachment of MUA on HAu electrode was confirmed with the presence of peaks at 558 cm^{-1} and 731 cm^{-1} assigned to stretch mode of C-S (formation of Au-S covalent bond). Bands at 1157 cm^{-1}, 2852 cm^{-1}, and 2916 cm^{-1} were observed for the alkyl chains in MUA. The band at 1201 cm^{-1} is identified as the C-OH stretch mode of the –COOH group of MUA. Symmetric and asymmetric COO^- and C=O stretch of –COOH were observed at 1222 cm^{-1} and 1308 cm^{-1}. Further, formation of NHS ester (spectrum (ii)) was confirmed by bands at 1088 cm^{-1}, 1250 cm^{-1}, 1365 cm^{-1}, 1750 cm^{-1}, 1793 cm^{-1}, and 1823 cm^{-1}. The bandat1088 cm^{-1} is due to the N-C-O stretch of NHS ester. A symmetric C-N-C stretch of NHS ester was observed at 1365 cm^{-1}. Peaks at 1750 cm^{-1} and 1793 cm^{-1} were observed for the C=O asymmetric and symmetric stretch of C=O carbonyls of NHS carbonyl respectively. Protein immobilization was confirmed by formation of –CO-NH amide bond (spectrum (iii)) as shown by the bands at 1552 cm^{-1} and 1674 cm^{-1}.

Estimation of bound protein (BSA) on HAu electrode

Table 1 represents quantitative estimation of immobilized protein on the surface functionalized HAu electrode. An indirect way of measurement was used to estimate the amount of immobilized protein on the HAu electrode. Unknown amount of protein found in the wash buffers of different sets of electrodes were estimated from the standard curve of BSA populated by Bradford assay. Bound protein was thus estimated by subtracting the amount of unbound protein from the originally incubated amount of protein. Binding efficiency of BSA on functionalized plain gold electrode was found to below (~28%) due to less surface area available as compared to high binding efficiency on functionalized HAu electrode (94%) that was primarily for the enhanced surface area due to nanotexturing. HAu electrode having no surface functionalization shows weak binding efficiency of protein, thus indicates that mere physisorption for binding protein on an electrode surface is not sufficient for sensing application.

Sensitivity performance HAu immunosensor

CV was performed on the HAu electrode immobilized with EGFR antibody followed by interaction of EGFR protein (Fig. 5) in equimolar solution (0.75 mM) of $K_3Fe(CN)_6$ and $K_4Fe(CN)_6$ in 0.1 M of KCl electrolyte. In coherence with previous results upon covalent immobilization of 500 ng/mL EGFR immunoglobulin protein on the sensing surface, a large suppression in current was observed in comparison to a pristine HAu electrode. Thereafter, binding affinity and sensitivity of EGFR immunoglobulin for EGFR protein (antigen) was measured by studying natural affinity between the Antibody-Antigen using different concentrations of EGFR antigen (ranging from 1 ng/mL to 10 pg/mL). Figure 5 shows a sharp

Table 1 — Bound Protein estimation on gold electrode using concentration of protein in wash buffer concentration

Type of Electrode	Amount of BSA incubated (A)	Amount of BSA leached in wash buffer (B)	Amount of BSA bound on electrode (A-B)	Binding efficiency E= (A-B)/A
Plain Gold with Surface functionalization	25 µg	17.9 µg	7.1 µg	28± 0.6%
HAu without surface functionalization	25 µg	24.5 µg	0.5 µg	2 ± 0.9%
HAu with surface functionalization	25 µg	1.5 µg	23.5 µg	94 ± 3%

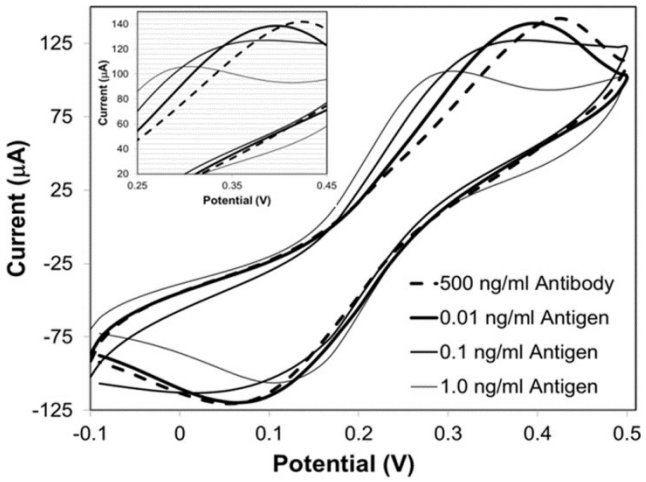

Fig. 5 — CV of $[Fe(CN)_6]^{3-/4-}$ electrolyte representing EGFR antibody-antigen interaction on the HAu electrode

reduction in the redox peak current with increase in antigen concentration. Suppression in the redox peak is an obvious indication of reduced electron transfer activity at the sensing surface of HAu electrode. Addition of antigen adds to insulating layers by forming antigen-antibody complex at the HAu electrode Thus, blocking more and more electron transfer between the electrodes.

Conclusion

Our entire study was primarily focused on improvement of the overall performance of the proposed affinity based HAu biosensor. In this context, we could demonstrate that the hierarchical and uniformly distributed gold nanostructures, that were electrodeposited by LSV in presence of optimum concentration of APTES additive showed an excellent surface coverage of protein molecules as high as 94%. In addition, surface functionalization using covalent binding on the HAu surface was quite rapid in comparison to that on a plain gold surface. As a result, protein immobilization on the HAu surface was also strong and effective as proven by the CV and FTIR analysis. We also demonstrated that these HAu electrodes are highly sensitive towards detection of proteins by employing Antibody-Antigen interaction where specifically EGFR antigen could be detected by EGFR antibody with a broad linear range of 1 ng/mL to 10 pg/mL. With such high sensitivity, there exists strong prospect for early detection of other protein biomarkers of cancer as well.

Acknowledgement

Authors thank Indian council of Medical research for funding (5/13/04/2015-NCD-III) this work.

Conflict of interest

All authors declare no conflict of interest.

References

1 Yankun L, Xinpeng M, Kenan H & Zhichao B, Applications of serum amino acid levels in identification of cancer. *Indian J Biochem Biophys*, 56 (2019) 53.

2 Giljohann DA & Mirkin CA, Drivers of biodiagnostic development. *Nature*, 462 (2009) 461.

3 Yang Z, Qiao L, Chao Y, Liu J, Di Y, Sun J, Zhang J, Huang L, Guo H & He C, High expression of nucleophosmin is closely related to the grade and invasion of colorectal cancer. *Indian J Biochem Biophys*, 56 (2019) 420.

4 Chattopadhyay K & Dipak, Antibacterial Metallopharmaceuticals: Into the Nanoscale Regime of Silver. *Antibact Met Into Nanoscale Regime Silver*, 01 (2010) 427.

5 Ludwig JA & Weinstein JN, Biomarkers in cancer staging, prognosis and treatment selection. *Nat Rev Cancer*, 5 (2005) 845.

6 Goodsaid FM & Mendrick DL, Translational medicine and the value of biomarker qualification. *Sci Transl Med*, 2 (2010) 47.

7 Yang Z, Qiao L, Chao Y, Liu J, Di Y, Sun J, et al. Antibacterial Metallopharmaceuticals: Into the Nanoscale Regime of Silver. *Antibact Met Into Nanoscale Regime Silver*, 01 (2010) 420.

8 Mohan IK, Sreedevi N, Baba KS, Bhaskar MV, Hussain T, Alrokayan SA & Naushad SM, Application of multiple linear regression and machine learning algorithms to elucidate the association of poor glycemic control and hyperhomocysteinemia with microalbuminuria. *Indian J Biochem Biophys*, 56 (2019) 150.

9 Pan S, Chen R, Brand RE, Hawley S, Tamura Y, Gafken PR, Milless BP, Goodlett DR, Rush J & Brentnall TA, Multiplex targeted proteomic assay for biomarker detection in plasma:

A pancreatic cancer biomarker case study. *J Proteome Res*, 11 (2012) 1937.
10 Urdea M, Penny LA, Olmsted SS, Giovanni MY, Kaspar P, Shepherd A, Wilson P, Dahl CA, Buchsbaum S, Moeller G & Burgess DCH, Requirements for high impact diagnostics in the developing world. *Nature*, 444 (2006) 73 Suppl 1.
11 Selvam P, Vijayakumar T, Wadhwani A & Muthulakshmi L, Bioreduction of silver nanoparticles from aerial parts of *Euphorbia hirta* L. (EH-ET) and its potent anticancer activities against neuroblastoma cell lines. *Indian J Biochem Biophys*, 56 (2019) 132.
12 Kale SK, Functionalization of Fe_3O_4 nanoparticles. *Indian J Pure Appl Phys*, 56 (2018) 728.
13 Wang EC & Wang AZ, Nanoparticles and their applications in cell and molecular biology. *Integr Biol* (*Camb*), 6 (2014) 9.
14 Leca-Bouvier B & Blum LJ, Biosensors for Protein Detection: A Review. *Anal Lett*, 38 (2005) 1491.
15 Grieshaber D, MacKenzie R, Vörös J & Reimhult E, Electrochemical Biosensors - Sensor Principles and Architectures. *Sensors*, 8 (2008) 1400.
16 Jans H & Huo Q, Gold nanoparticle-enabled biological and chemical detection and analysis. *Chem Soc Rev*, 41 (2012) 2849.
17 Liu D, Wang Z & Jiang X, Gold nanoparticles for the colorimetric and fluorescent detection of ions and small organic molecules. *Nanoscale*. 3 (2011) 1421.
18 Conde J, Dias JT, Grazú V, Moros M, Baptista PV & de la Fuente JM, Revisiting 30 years of biofunctionalization and surface chemistry of inorganic nanoparticles for nanomedicine. *Front Chem*, 2 (2014) 1.
19 Wilson R, The use of gold nanoparticles in diagnostics and detection. *Chem Soc Rev*, 37 (2008) 2028.
20 Lewinski N, Colvin V & Drezek R, Cytotoxicity of nanopartides. *Small*, 4 (2008) 26.
21 Paciotti GF, Myer L, Weinreich D, Goia D, Pavel N, McLaughlin RE & Tamarkin L, Colloidal gold: A novel nanoparticle vector for tumor directed drug delivery. *Drug Deliv*, 11 (2004) 169.
22 Jiao PF, Y. Zhou H, Chen LX & Yan B, Cancer-targeting multifunctionalized gold nanoparticles in imaging and therapy. *Curr Med Chem*, 18 (2012) 2086.
23 Soleymani L, Fang Z, Sun X, Yang H, Taft BJ, Sargent EH & Kelley SO, Nanostructuring of patterned microelectrodes to enhance the sensitivity of electrochemical nucleic acids detection. *Angew Chemie Int Ed Engl*, 48 (2009) 8457.
24 Tian Y, Liu H, Zhao G & Tatsuma T, Shape-Controlled Electrodeposition of Gold Nanostructures. *J Phys Chem B*, 110 (2006) 23478.
25 Guo S, Wang L & Wang E, Templateless, surfactantless, simple electrochemical route to rapid synthesis of diameter-controlled 3D flowerlike gold microstructure with "clean" surface. *Chem Commun*, 30 (2007) 3163.
26 Zhang X, Shi F, Yu X, Liu H, Fu Y, Wang Z, Jiang L & Li X, Polyelectrolyte Multilayer as Matrix for Electrochemical Deposition of Gold Clusters: Toward Super-Hydrophobic Surface. *J Am Chem Soc* 126 (2004) 3064.
27 Sepulveda D, Aroca MA, Varela A, Del Portillo P & Osma JF, Bioelectrochemical detection of mycobacterium tuberculosis ESAT-6 in an antibody-based biomicrosystem. *Sensors* (*Basel*), 17 (2017) 2178.
28 Tuttle IV PV, Rundell AE & Webster TJ, Influence of biologically inspired nanometer surface roughness on antigen-antibody interactions for immunoassay-biosensor applications. *Int J Nanomed*, 1 (2006) 497.
29 Nayak R & Knapp DR, Matrix-Free LDI mass spectrometry platform using patterned nanostructured gold thin film. *Anal Chem*, 82 (2010) 7772.
30 Ngunjiri JN, Stark DJ, Tian T, Briggman KA & Garno JC, Immobilization of proteins on carboxylic acid functionalized nanopatterns. *Anal Bioanal Chem*, 405 (2013) 1985.
31 Jordon CE, Frey BL, Kornguth S, Corn RM. Characterization of poly-L-lysine adsorption onto alkanethiol-modified gold surfaces with polarization-modulation Fourier transform infrared spectroscopy and surface plasmon resonance measurements. *Langmuir*, 10 (1994) 3642.
32 Moldovan C, Mihailescu C, Stan D, Ruta L, Iosub R, Gavrila R, Puricaa M & Vasilica S, Characterization of self-assembled monolayers (SAMs) on silicon substrate comparative with polymer substrate for Escherichia coli O157:H7 detection. *Appl Surf Sci*, 225 (2009) 8953.